

# Target Tracking of an Underwater Glider Using a Small Unmanned Surface Vessel

Ivar Bjørge Saksvik\* Alex Alcocer\* Vahid Hassani\*\*  
Antonio Pascoal\*\*\*

\* *Department of Mechanical, Electronics and Chemical Engineering,  
Oslo Metropolitan University, Oslo, Norway (e-mail:  
s309664@oslomet.no, alepen@oslomet.no, vahid.hassani@oslomet.no).*

\*\* *Department of Ships and Ocean Structures, SINTEF Ocean,  
Trondheim, Norway (e-mail: vahid.hassani@sintef.no).*

\*\*\* *Laboratory of Robotics and Systems in Engineering and Science  
(LARSyS), ISR/IST, University of Lisbon, Lisbon, Portugal  
antonio@tecnico.ulisboa.pt*

**Abstract:** This paper proposes a methodology for target tracking of an underwater glider using an *unmanned surface vessel* (USV). The topside USV is assumed to have knowledge about the position of the underwater glider from an acoustic positioning system, which is exploited to track the planar motions of the submerged vehicle from the surface. We propose a target tracking method for the purpose of glider localization using unmanned systems to reduce the operational costs and potential hazards. A guidance law is implemented on the topside vehicle to track the submerged vehicle when the latter performs generic glider manoeuvres. A numerical simulation environment of the two vehicles is presented to validate the target-tracking scheme.

Copyright © 2022 The Authors. This is an open access article under the CC BY-NC-ND license (<https://creativecommons.org/licenses/by-nc-nd/4.0/>)

**Keywords:** Target tracking, Underwater Glider, Unmanned Surface Vehicle (USV).

## 1. INTRODUCTION

Navigation systems onboard underwater gliders are often prone to estimation errors due to limited sensor payloads. In practice, inertial measurement units (IMUs) and depth sensors are used to approximate the position of the glider through simple kinematic equations, which frequently leads to navigation errors. Absence of accurate position estimates makes it challenging to implement and evaluate the performance of guidance, navigation, and control (GNC) systems. To obtain accurate estimates of glider trajectories, an acoustic baseline positioning system is typically employed as demonstrated in Graver et al. (2003) and Bahr et al. (2009). In practice, however, this requires cumbersome and costly deployment and calibration of several transponders on the seabed. This paper proposes a strategy to estimate such trajectories using an unmanned surface vessel equipped with a low-power acoustic positioning system with limited calibration requirements. Due to range limitations in low-power acoustics, it is convenient to bound the planar distance between the topside vessel (equipped with acoustic receivers) and the submerged vehicle carrying an acoustic transmitter. From a control perspective, we call this a *target-tracking* problem, where the goal is to pursue a moving target, whose future motion is not known. The objective of this paper is to let the topside vessel track the motions of

the submerged glider so that the planar distance between the two vehicles is reduced. This motion control problem has been introduced in several underwater tracking & localization schemes using one or more autonomous surface vessels (ASVs), see e.g., Hung et al. (2021), Moreno-Salinas et al. (2016), Hung et al. (2020), Norgren et al. (2015). The manoeuvring task for the topside vessel in combined tracking and localization of underwater vehicles is highly dependent on the number of range-measurements available. For instance, single-beacon vehicles, limited to one acoustic range measurement, impose a challenge of trilaterate the position of an underwater vehicle. The latter issue is solved in Moreno-Salinas et al. (2016) and Masmijja et al. (2018) by continuously encircling about the moving target to increase the range-based information. In this paper we assume that the topside vessel has enough acoustic receivers (a short baseline setup) to localize the target carrying the transmitter, without the need of additional motion planning (e.g., encircling about the target). Moreover, a vectorial guidance law is proposed for the USV to track generic motions of an underwater glider. Due to underactuated vessel dynamics the guidance law is decomposed to surge and heading controllers to relax the dynamic and kinematic assignments of the target-tracking scheme respectively.

The paper is organized as follows: The target-tracking guidance law and maneuvering model of the topside vessel is derived in section 2 and 3 respectively. The target, an underwater glider, is detailed in section 4. Simulation results are presented in section 5 and recommendations for further work are presented in section 6.

\* This work was supported by the OASYS project funded by the Research Council of Norway (RCN), the German Federal Ministry of Economic Affairs and Energy (BMWi) and the European Commission under the framework of the ERA-NET Cofund MarTERA.

## 2. TARGET TRACKING GUIDANCE LAW

Methods originally developed in the context of airborne guidance systems have been extended to marine vessels, see for example Breivik and Fossen (2007), Breivik et al. (2008), Norgren et al. (2015), and Skejic et al. (2009). In this section we derive a constant bearing (CB) guidance law based on the theory presented in the latter works. Following the notation in Breivik et al. (2008), we refer to the surface vessel as the *interceptor* and the underwater glider as the *target*, which yields the following assumptions:

**Assumption 2.1:** *The subsequent vectorial definitions are specified with respect to a fixed local frame denoted  $\{n\}$  with the origin located at an arbitrary point.*

**Assumption 2.2:** *The target is assumed to have a non-zero speed denoted  $U_t^n$  satisfying  $U_t^n(t) > 0 \forall t$*

**Assumption 2.3:** *The proposed guidance law considers a target moving in a planar plane, thus neglecting vertical motions*

**Remark 2.1:** *Assumption 2.1 implies the interceptor have no information about the target's motion in the body-fixed frame  $\{b\}$ . Secondly, the origin of the fixed local frame  $\{n\}$  is chosen by the control operator, typically somewhere close the operation area Penas (2009)*

The proposed constant bearing (CB) guidance law is derived from a geometric view of the target and interceptor. Following assumption 2.2, we define the planar distance between the target  $\mathbf{P}_t^n \in \mathbb{R}^2$  and interceptor  $\mathbf{P}_u^n \in \mathbb{R}^2$  as

$$\hat{\mathbf{P}}_n = (\mathbf{P}_t^n - \mathbf{P}_u^n) = \begin{bmatrix} x_t^n - x_u^n \\ y_t^n - y_u^n \end{bmatrix} \quad (1)$$

Differentiating  $\mathbf{P}_t^n$  and  $\mathbf{P}_u^n$  with respect to time yields the inertial velocities  $\boldsymbol{\nu}_t^n = [\dot{x}_t^n, \dot{y}_t^n]^T$  and  $\boldsymbol{\nu}_u^n = [\dot{x}_u^n, \dot{y}_u^n]^T$ . Following Breivik et al. (2008), the CB guidance law is presented as a velocity assignment denoted by  $\boldsymbol{\nu}_d^n = [\dot{x}_d^n, \dot{y}_d^n]^T$ , given by

$$\boldsymbol{\nu}_d^n = (\boldsymbol{\nu}_t^n + \boldsymbol{\nu}_a^n) \quad (2)$$

where  $\boldsymbol{\nu}_a \in \mathbb{R}^2$  is the desired approach velocity vector, derived by a maximum approach speed  $\bar{U}_a$  and a transient control parameter  $\Lambda$ , yielding

$$\boldsymbol{\nu}_a^n = \bar{U}_a \cdot \frac{\hat{\mathbf{P}}_n}{\sqrt{\hat{\mathbf{P}}_n^T \cdot \hat{\mathbf{P}}_n + \Lambda^2}} \in \mathbb{R}^2 \quad (3)$$

The maximum approach speed  $\bar{U}_a^n$  must be chosen carefully according to maneuverability considerations and physical limitations of the USV.

Most marine vessels are underactuated and for this reason the sway dynamics cannot be controlled directly during nominal operations. Thus, we cannot request the vessel to track a desired arbitrary velocity vector. However, as demonstrated in Breivik et al. (2008), the CB guidance law is decomposed into surge and heading controllers that control the magnitude and direction of the velocity vector, respectively. We reformulate the velocity assignment in eq. 2 to a speed assignment  $U_d^n = \sqrt{(\dot{x}_d^n)^2 + (\dot{y}_d^n)^2}$ . Furthermore, the control objective becomes

$$\lim_{t \rightarrow \infty} (U_d^n - U_u^n) = 0 \quad (4)$$

where  $U_u^n$  is the speed of the vessel. It is convenient to assume that the desired sway motions are small, satisfying  $\dot{x}_d^n \gg \dot{y}_d^n$ , and that

$$u_d^b \approx U_d^n \quad (5)$$

This then introduces a new control objective

$$\lim_{t \rightarrow \infty} (u_d^b - u_u^b) = 0 \quad (6)$$

where  $u_u^b$  is the surge velocity of the vessel in the body-fixed frame  $\{b\}$ .

A *line-of-sight* (LOS) guidance law is proposed to control the direction of the desired velocity vector  $\boldsymbol{\nu}_d^n$ . Following Skejic et al. (2009) and Breivik and Fossen (2009), the LOS guidance law is geometrically represented by the relative position of the vessel with respect to the target  $\mathbf{P}_t^n$ . The relative position between the two vehicles is formulated by a cross-track error  $y_e^n$ ,

$$y_e^n = -(x_u^n - x_t^n) \cdot \sin(\chi_t) + (y_u^n - y_t^n) \cdot \cos(\chi_t) \quad (7)$$

where  $\chi_t = \text{atan2}(\dot{y}_t^n, \dot{x}_t^n) \in [-\pi, \pi]$  is the target course angle. The LOS guidance law is derived using a *look-ahead* distance parameter  $\lambda$  which determines the transient convergence towards the target, lying a "a head" of the interceptor. From Skejic et al. (2009) the LOS guidance law is given as the course angle reference

$$\chi_{LOS} = \tan^{-1}\left(\frac{-y_e^n}{\lambda}\right) \quad (8)$$

which is further rewritten as the heading reference

$$\psi_{LOS} = (\chi_{LOS} + \chi_t) - \beta_u \quad (9)$$

where  $\beta_u = \text{asin}(v_u^b/U_u^b)$  is the sideslip angle of the interceptor. Finally, the control objective for the heading controller becomes

$$\lim_{t \rightarrow \infty} (\psi_{LOS} - \psi_u) = 0 \quad (10)$$

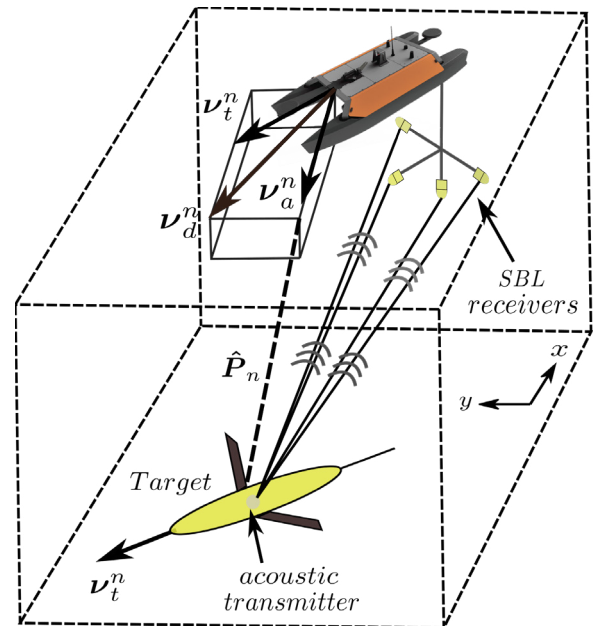


Figure 1. Illustration of the target tracking problem and corresponding vectors for the CB guidance law

### 3. USV MODEL

This section describes the mathematical model of the topside vessel. The vehicle simulated in this paper is an *Otter USV* developed by Maritime Robotics. The vehicle is characterized as a small unmanned catamaran as illustrated in figure 2. We first introduce some assumptions about the vehicle

**Assumption 3.1:** *Environmental wind and wave loads acting on the vessel  $\tau_{wind}, \tau_{wave}$  are neglected*

**Assumption 3.2:** *The payload (acoustic receiver antenna) hydrodynamic drag and added mass effects are neglected*

**Assumption 3.3:** *The vessel is influenced by an ocean current  $\mathbf{V}_c^n = [V_x, V_y, 0]^T$  which is considered constant and irrotational in the inertial frame, hence  $\dot{\mathbf{V}}_c^n = 0$ .*

**Assumption 3.4:** *The hydrodynamic damping of the vessel is considered linear*



Figure 2. Maritime Robotics Otter USV with Waterlinked short-baseline (SBL) acoustic antenna/receivers, courtesy of OsloMet

The USV kinematics are defined by the state vector  $\boldsymbol{\eta} = [x, y, \psi]^T$ , consisting of the inertial position and the heading (yaw)  $\psi$  of the vessel. The kinematic equations are defined in terms of a rotation matrix  $\mathbf{R}_b^n(\psi)$  from the body-frame  $\{b\}$  to the inertial frame  $\{n\}$ , given by

$$\mathbf{R}_b^n(\psi) \triangleq \begin{bmatrix} c(\psi) & -s(\psi) & 0 \\ s(\psi) & c(\psi) & 0 \\ 0 & 0 & 1 \end{bmatrix}, \in SO(3) \quad (11)$$

where  $c = \cos()$  and  $s = \sin()$ . The dynamics are defined in terms of evolution of the surge  $u$  and sway  $v$  velocities and the yaw rate  $r$ , forming the state vector  $\boldsymbol{\nu} = [u, v, r]^T$ . Following assumption 3.3 there exists a constant irrotational ocean current vector in the planar plane. We rewrite the latter state vector into a relative velocity vector following Fossen (2011),  $\boldsymbol{\nu}_r = [u_r, v_r, r]^T = [u - u_c^b, v - v_c^b, r]^T$ , where  $u_c^b$  and  $v_c^b$  are the ocean currents described in the body-fixed frame  $\{b\}$ , derived as

$$\boldsymbol{\nu}_c^b = \begin{bmatrix} V_c^n \cdot \cos(\beta_c - \psi) \\ V_c^n \cdot \sin(\beta_c - \psi) \\ 0 \end{bmatrix}, V_c^n = \sqrt{u_c^n + v_c^n} \quad (12)$$

and  $\beta_c$  is the direction of the ocean current. Following Fossen (2011) the USV dynamics and kinematics (3DOF) are derived as

$$\dot{\boldsymbol{\eta}} = \mathbf{R}(\psi)\boldsymbol{\nu}_r + \mathbf{V}_c^n \quad (13)$$

$$\mathbf{M}\dot{\boldsymbol{\nu}}_r + \mathbf{C}(\boldsymbol{\nu}_r)\boldsymbol{\nu}_r + \mathbf{D}(\boldsymbol{\nu}_r)\boldsymbol{\nu}_r = \boldsymbol{\tau}_c \quad (14)$$

where  $\mathbf{M} = \mathbf{M}_{rb} + \mathbf{M}_A$  and  $\mathbf{C}(\boldsymbol{\nu}_r) = \mathbf{C}_{rb}(\boldsymbol{\nu}_r) + \mathbf{C}_A(\boldsymbol{\nu}_r)$  are the translational and rotational rigid-body dynamics with corresponding added mass effects. Hydrodynamic forces and moments are included in the damping matrix  $\mathbf{D}(\boldsymbol{\nu}_r)$ . Control forces and moments which act on the vessel are defined by  $\boldsymbol{\tau}_c = \mathbf{BK}\mathbf{u} = [\tau_u, 0, \tau_r]^T$ , where  $\mathbf{B}$  is the actuator configuration matrix which maps the control inputs (thruster revolutions)  $\mathbf{u} = [T_u, 0, T_r]^T$  into surge forces and yaw moments.  $\mathbf{K}$  is the diagonal force coefficient matrix. The matrices  $\mathbf{M}, \mathbf{C}, \mathbf{B}, \mathbf{D}$  can be written as

$$\mathbf{M} \triangleq \begin{bmatrix} m_{11} & 0 & 0 \\ 0 & m_{22} & m_{23} \\ 0 & m_{32} & m_{33} \end{bmatrix}, \mathbf{B} \triangleq \begin{bmatrix} b_{11} & b_{12} \\ 0 & 0 \\ b_{31} & b_{32} \end{bmatrix} \quad (15)$$

$$\mathbf{C} \triangleq \begin{bmatrix} 0 & 0 & c_{13} \\ 0 & 0 & c_{23} \\ c_{31} & c_{32} & 0 \end{bmatrix}, \mathbf{D} \triangleq \begin{bmatrix} d_{11} & 0 & 0 \\ 0 & d_{22} & d_{23} \\ 0 & d_{32} & d_{33} \end{bmatrix}$$

The Otter USV is actuated by two *nonrotatable* aft thrusters which implies that the control allocation problem is trivial and unconstrained. Furthermore, the control inputs of the two thrusters  $\mathbf{u} = [T_u, T_r]^T$  are computed by reducing  $\mathbf{B}, \mathbf{K}, \mathbf{u}$  to  $\mathbb{R}^2$ , such that

$$\mathbf{u} = \mathbf{K}^{-1} \mathbf{B}^{-1} \boldsymbol{\tau}_c \quad (16)$$

Following Paliotta et al. (2018) we derive the kinematic and dynamic equations derived in eq. 3 into component form as

$$\begin{aligned} \dot{x} &= u_r \cdot c(\psi) - v_r \cdot s(\psi) + V_x^n \\ \dot{y} &= v_r \cdot s(\psi) - v_r \cdot c(\psi) + V_y^n \\ \dot{\psi} &= r \\ \dot{r} &= F_r(u_r, v_r, r) + \tau_r \\ \dot{u}_r &= F_{u_r}(v_r) + \tau_u \\ \dot{v}_r &= X(u_r) + Y(u_r) \cdot v_r \end{aligned} \quad (17)$$

where the functions  $F_r(u_r, v_r, r), F_{u_r}(u_r), X(u_r), Y(u_r)$  are defined in the Appendix. From assumption 3.4 we have that the terms  $X(u_r)$  and  $Y(u_r)$  are linear.

The control objective for the USV is to track a moving vehicle whose future motions are not known. The target tracking reference is defined by  $\boldsymbol{t}_d = [x_d, y_d, \psi_d, u_d]^T$ , which represents the desired planar position, heading and surge velocity. Consequently, we want to relax the following conditions

$$\begin{aligned} \lim_{t \rightarrow \infty} (x_u^n - x_t^n) &= 0, \quad \lim_{t \rightarrow \infty} (y_u^n - y_t^n) = 0 \\ \lim_{t \rightarrow \infty} (\psi - \psi_{LOS}) &= 0, \quad \lim_{t \rightarrow \infty} (u_u^b - u_d^b) = 0 \end{aligned} \quad (18)$$

**Remark 3.1** *The control objectives imply that the vessel is underactuated as we want to control 3DOF with only two control inputs  $\mathbf{u} \in \mathbb{R}^2$*

#### 3.1 Control System

The proposed target-tracking guidance law in section 2 computes references for surge and heading controllers. Following assumption 3.4 we introduce two model based PID controllers with feedforward reference terms. We linearize the maneuvering model in eq. 3 to 1DOF heading and surge subsystems (*Nomoto models*). A PI controller and a PID controller are proposed for surge and heading control, respectively. Given the control errors  $\hat{u} = (u - u_d)$

and  $\hat{\psi} = (\psi - \psi_d)$ , the model-based controllers are defined by

$$\begin{aligned}\tau_u &= (m - X_{\dot{u}})\dot{u}_d + X_u u_d - k_{p_u} \hat{u} - k_{i_u} \int_0^t \hat{u}(\tau) d\tau \\ \tau_r &= (I_z - N_{\dot{r}})\dot{\psi}_d + N_r \psi_d - k_{p_\psi} \hat{\psi} - k_{d_\psi} \dot{\hat{\psi}} - K_{i_\psi} \int_0^t \hat{\psi}(\tau) d\tau\end{aligned}\quad (19)$$

where  $X_{\dot{u}}, X_u, N_{\dot{r}}, N_r$  are the hydrodynamic damping forces/moments and their derivatives (added mass) in surge and yaw and  $m$  and  $I_z$  are the vehicle mass and inertia (vertical component) respectively.

#### 4. TARGET - UNDERWATER GLIDER

The target, an autonomous underwater glider (shown in figure 1), is a special class of autonomous underwater vehicles (AUVs). The glider's main source of locomotion is a variable buoyancy system (VBS) which allows the vehicle to move up and down in the water column. A set of fixed wings attached to the glider body transform the vertical motions into forward movement from the horizontal component of the hydrodynamic lift force (vertical force). The absence of aft thrusters ensures longevity in glider missions as documented in various field experiments Glenn et al. (2011), Webb et al. (2001). In Elkolali et al. (2022) a novel miniaturized underwater glider is developed as illustrated in figure 3.



Figure 3. OASYS underwater glider (Elkolali et al. (2022)), courtesy of OsloMet

Due to slow cruising speeds, conventional control surfaces are replaced by an internal moving mass system. This typically consists of a custom shaped battery-pack that can be translated and rotated inside the glider housing, see Zhang et al. (2013), Mahmoudian and Woolsey (2008), Saksvik et al. (2021). The moving mass actuators create pitch and yaw moments for attitude and heading control.

The steady-state flight characteristics of underwater gliders are twofold. If the vehicle is stable in roll (wings-levelled), they perform repeating saw-tooth manoeuvres with non-zero pitch angles and a fixed heading. Seen from the surface (2D), the trajectory is viewed as a straight-line. The second flight is a vertical spiral which is analogous to how fixed-winged aerial vehicles turn. Turning is induced if the rotating mass actuator is shifted. Accordingly, a roll moment is applied such that the wings are no longer aligned horizontally. The spiral manoeuvre is characterized as a circle seen from the topside vehicle. The goal of the topside vessel is to pursuit these generic glider manoeuvres, consisting of both straight-line and curved trajectories.

#### 5. SIMULATION & RESULTS

To validate the proposed target tracking scheme, a dual simulation environment of the target (underwater glider) and interceptor (USV) was developed. The mathematical model of the Otter USV was implemented using the MSS (Marine System Simulator) toolbox Perez et al. (2006) developed following the guidelines in Fossen (2011). The simulated glider object is the *Seawing glider* presented in Zhang et al. (2013). This is a research glider which has similar shape and actuator configuration as the OASYS glider in figure 3. The attitude and heading is controlled using internal moving and rotating mass actuators. This consists of a cylindrical battery-pack which can be translated and rotated inside the vehicle housing. Furthermore, the net buoyancy is controlled by an oil distribution system with flexible bladders to manipulate the volume displacement of the vehicle. The dynamics of the USV and underwater glider were implemented in Simulink for simultaneous simulation, together with the constant bearing guidance law and control system presented in section 2 and 3 respectively. The mathematical model of the simulated glider is presented in Saksvik et al. (2021).

##### 5.1 Simulation parameters

Due to the slow cruising speeds in underwater gliders, we set the max approach speed in the CB guidance law as  $\bar{U}_a^n = 0.7 \text{ m/s}$ . Furthermore, the transient control parameter was set to  $\Lambda = 10$ . For the planar motion LOS guidance law, the look-ahead distance is  $\lambda = 5$  meters. The PID terms for the surge and heading controllers in eq. 19 are tuned by a pole-placement algorithm. We reuse the PID-terms for the Otter USV as presented in the MSS toolbox Perez et al. (2006) / Fossen (2011) and Torvund (2020).

Controller	$k_p$	$k_i$	$k_d$
Surge (Torvund (2020))	239	47	
Heading (Fossen (2011))	300	1	10

We present two general simulation cases for the target tracking application. These consists of a vertical spiral where the USV follows a circle from the surface, and a saw-tooth trajectory which results in a straight-line target tracking problem for the topside vehicle. During these simulations, there exists an ocean current with magnitude  $V_c^n = \sqrt{u_c^n + v_c^n} = 0.15 \text{ m/s}$  and direction  $\beta_c = \frac{\pi}{2} \text{ rad}$ . In the first simulation case the initial position and heading of the USV is given as  $[x_0, y_0, \psi_0] = [0, -30, 0]^T$ . The initial state for the underwater glider is  $[x_0, y_0, \psi_0]^T = [0, 0, 0]^T$ . Seen from the surface, the USV is initially located 30 meters off east with respect to the underwater glider, which is located at the origin of the inertial frame. The initial heading of the two vehicles coincides.

In the second case study we investigate a straight-line target tracking problem. In this simulation case, the USV is initialized with an offset planar position and heading with respect to the glider. The following initial conditions are considered for the USV  $[x_0, y_0, \psi_0] = [-100, -35, -\frac{\pi}{2}]^T$ . Moreover, the initial conditions of the glider is the same as case 1:  $[x_0, y_0, \psi_0]^T = [0, 0, 0]^T$ .

5.2 Case 1 - Curved target tracking

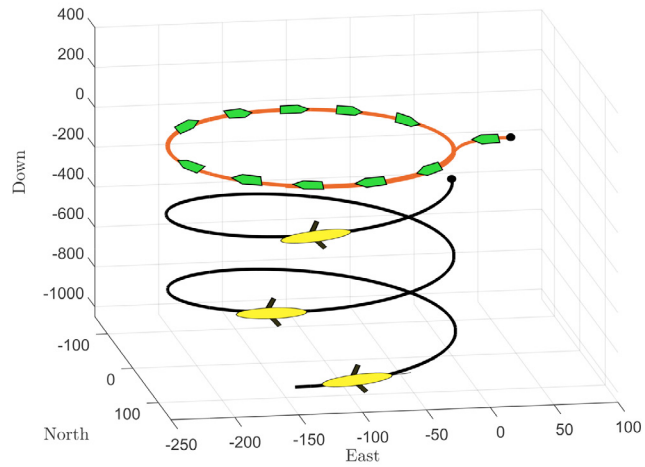


Figure 4. Tracking a circular motion

5.3 Case 2 - Straight line target tracking

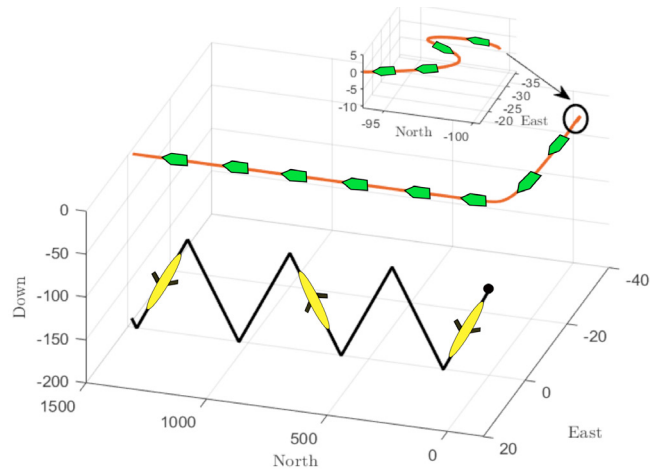


Figure 7. Straight-line target tracking

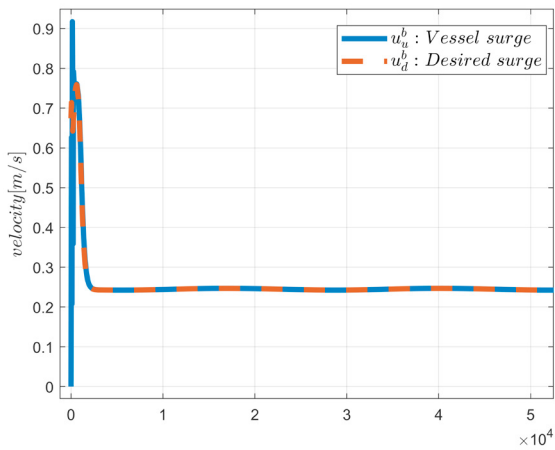


Figure 5. Surge control - Case 1

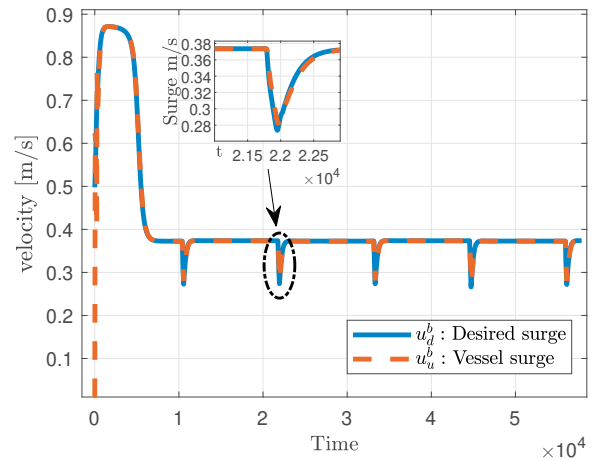


Figure 8. Surge control - Case 2

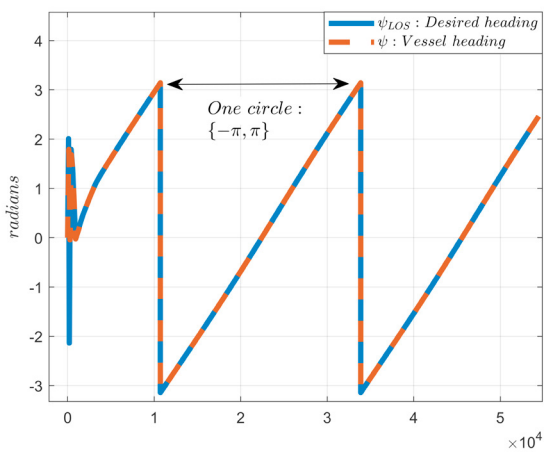


Figure 6. Heading autopilot - Case 1

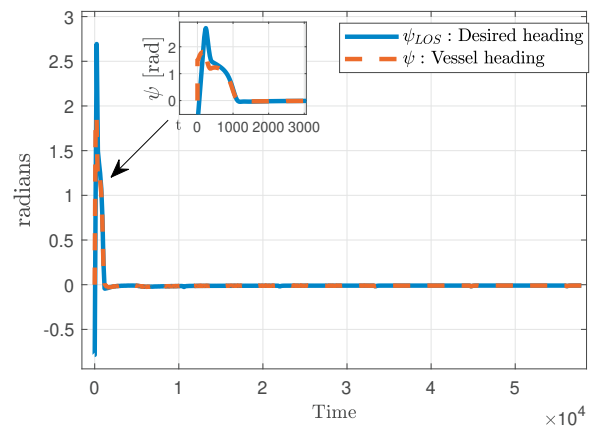


Figure 9. Heading autopilot - Case 2

## 6. CONCLUSION & FURTHER WORK

This paper proposed a target-tracking scheme of underwater gliders using a USV. A constant bearing guidance law was presented to pursuit the motions of the submerged glider from the surface. Simulation results show tracking convergence for generic glider manoeuvres. However, full scale experiments must be carried for further validation. The extension of this work is to validate the proposed target tracking scheme via experimental tests. The aim is to use an Otter USV and OASYS glider owned by the ocean laboratory (Oceanlab) at Oslo Metropolitan University. The topside vessel is complemented by a short baseline (SBL) acoustic positioning system from Waterlinked.

## 7. APPENDIX

The terms  $F_{u_r}(u_r)$ ,  $X(u_r)$ ,  $Y(u_r)$ ,  $F_r(u_r, v_r, r)$  are defined in this appendix. From Paliotta et al. (2018) we have the following definitions

$$\begin{aligned} F_{u_r}(v_r, r) &\triangleq \frac{1}{m_{11}} (m_{22} v_r + m_{23} r) r - \frac{d_{11}}{m_{11}} u_r \\ X(u_r) &\triangleq -\frac{m_{11} m_{33} - m_{23}^2}{m_{22} m_{33} - m_{23}^2} u_r + \frac{d_{33} m_{23} - d_{23} m_{33}}{m_{22} m_{33} - m_{23}^2} \\ Y(u_r) &\triangleq -\frac{(m_{11} - m_{22}) m_{23}}{m_{22} m_{33} - m_{23}^2} u_r - \frac{d_{22} m_{33} - d_{32} m_{23}}{m_{22} m_{33} - m_{23}^2} \\ F_r(u_r, v_r, r) &\triangleq \frac{m_{23} d_{22} - m_{22} (d_{32} + (m_{22} - m_{11}) u_r)}{m_{22} m_{33} - m_{23}^2} \cdot v_r \\ &\quad + \frac{m_{23} (d_{23} + m_{11} u_r) - m_{22} (d_{33} + m_{23} u_r)}{m_{22} m_{33} - m_{23}^2} r \end{aligned} \quad (20)$$

**Remark 7.1** The terms  $Y(u_r)$  and  $X(u_r)$  are assumed to be linear. Furthermore,  $Y(u_r)$  have the following bounds:

$$\frac{(m_{11} - m_{22}) m_{23}}{m_{22} m_{33} - m_{23}^2} u_r > 0, \quad \frac{d_{22} m_{33} - d_{32} m_{23}}{m_{22} m_{33} - m_{23}^2} > 0 \quad (21)$$

## REFERENCES

- Bahr, A., Leonard, J.J., and Fallon, M.F. (2009). Cooperative localization for autonomous underwater vehicles. *The International Journal of Robotics Research*, 28(6), 714–728.
- Breivik, M. and Fossen, T.I. (2007). Applying missile guidance concepts to motion control of marine craft. *IFAC Proceedings Volumes*, 40(17), 349–354.
- Breivik, M. and Fossen, T.I. (2009). Guidance laws for autonomous underwater vehicles. *Underwater vehicles*, 4, 51–76.
- Breivik, M., Hovstein, V.E., and Fossen, T.I. (2008). Straight-line target tracking for unmanned surface vehicles.
- Elkolali, M., Al-Tawil, A., and Alcocer, A. (2022). Design and testing of a miniature variable buoyancy system for underwater vehicles. *IEEE Access*, 10, 42297–42308.
- Fossen, T.I. (2011). *Handbook of marine craft hydrodynamics and motion control*. John Wiley & Sons.
- Glenn, S., Schofield, O., Kohut, J., McDonnell, J., Ludescher, R., Seidel, D., Aragon, D., Haskins, T., Handel, E., Haldeman, C., et al. (2011). The trans-atlantic slocum glider expeditions: A catalyst for undergraduate participation in ocean science and technology. *Marine Technology Society Journal*, 45(1), 52–67.
- Graver, J.G., Bachmayer, R., Leonard, N.E., and Fratantoni, D.M. (2003). Underwater glider model parameter identification. In *Proc. 13th Int. Symp. on Unmanned Untethered Submersible Technology (UUST)*, volume 1, 12–13.
- Hung, N.T., Crasta, N., Moreno-Salinas, D., Pascoal, A.M., and Johansen, T.A. (2020). Range-based target localization and pursuit with autonomous vehicles: An approach using posterior crlb and model predictive control. *Robotics and Autonomous Systems*, 132, 103608.
- Hung, N.T., Rego, F.F., and Pascoal, A.M. (2021). Co-operative distributed estimation and control of multiple autonomous vehicles for range-based underwater target localization and pursuit. *IEEE Transactions on Control Systems Technology*.
- Mahmoudian, N. and Woolsey, C. (2008). Underwater glider motion control. In *2008 47th IEEE Conference on Decision and Control*, 552–557. IEEE.
- Masmitja, I., Gomariz, S., Del-Rio, J., Kieft, B., O’Reilly, T., Bouvet, P.J., and Aguzzi, J. (2018). Optimal path shape for range-only underwater target localization using a wave glider. *The International Journal of Robotics Research*, 37(12), 1447–1462.
- Moreno-Salinas, D., Crasta, N., Ribeiro, M., Bayat, B., Pascoal, A., and Aranda, J. (2016). Integrated motion planning, control, and estimation for range-based marine vehicle positioning and target localization. *IFAC-PapersOnLine*, 49(23), 34–40.
- Norgren, P., Ludvigsen, M., Ingebretsen, T., and Hovstein, V.E. (2015). Tracking and remote monitoring of an autonomous underwater vehicle using an unmanned surface vehicle in the trondheim fjord. In *OCEANS 2015-MTS/IEEE Washington*, 1–6. IEEE.
- Paliotta, C., Lefeber, E., Pettersen, K.Y., Pinto, J., Costa, M., et al. (2018). Trajectory tracking and path following for underactuated marine vehicles. *IEEE Transactions on Control Systems Technology*, 27(4), 1423–1437.
- Penas, A.A. (2009). Positioning and navigation systems for robotic underwater vehicles. *Doctor thesis, Instituto Superior Tecnico*.
- Perez, T., Smogeli, O., Fossen, T., and Sorensen, A. (2006). An overview of the marine systems simulator (mss): A simlink toolbox for marine control systems. *Modeling, identification and Control*, 27(4), 259–275.
- Saksvik, I.B., Alcocer, A., and Hassani, V. (2021). A deep learning approach to dead-reckoning navigation for autonomous underwater vehicles with limited sensor payloads. *arXiv preprint arXiv:2110.00661*.
- Skejic, R., Breivik, M., Fossen, T.I., and Faltinsen, O.M. (2009). Modeling and control of underway replenishment operations in calm water. *IFAC Proceedings Volumes*, 42(18), 78–85.
- Torvund, P.G.B. (2020). *Nonlinear Autonomous Docking and Path-Following Control Systems for the Otter USV*. Master’s thesis, NTNU.
- Webb, D.C., Simonetti, P.J., and Jones, C.P. (2001). Slocum: An underwater glider propelled by environmental energy. *IEEE Journal of oceanic engineering*, 26(4), 447–452.
- Zhang, S., Yu, J., Zhang, A., and Zhang, F. (2013). Spiraling motion of underwater gliders: Modeling, analysis, and experimental results. *Ocean Engineering*, 60, 1–13.